HHS Public Access

Author manuscript

Horm Behav. Author manuscript; available in PMC 2021 May 18.

Published in final edited form as:

Horm Behav. 2021 January ; 127: 104887. doi:10.1016/j.yhbeh.2020.104887.

Inhibition of progesterone receptor activity during development increases reelin-immunoreactivity in Cajal-Retzius cells, alters synaptic innervation in neonatal dentate gyrus, and impairs episodic-like memory in adulthood

Andrew J. Newell, **Sung Hwan Chung**, **Christine K. Wagner***

Department of Psychology, University at Albany, Albany, NY 12222, United States of America

Center for Neuroscience Research, University at Albany, Albany, NY 12222, United States of America

Abstract

Progesterone receptor (PR) is expressed in Cajal-Retzius (CR) cells of the dentate gyrus (DG) molecular layer during the postnatal period (P1–28), a critical stage of development for the dentate gyrus and its circuitry. CR cells secrete the glycoprotein, reelin, which is required for typical development of the DG and its connections, particularly afferent input from the perforant path. This pathway regulates the processing of sensory information arriving from entorhinal cortex and integrates this information to form episodic memories. To assess the potential role of PR activity on the development of these connections and associated behavior, rats were treated daily from P1 to 7 with the PR antagonist, RU486. RU486 treatment increased the number of reelin-ir cells, suggesting an accumulation of reelin, and implicating PR in the regulation of a principle developmental function of CR cells. RU486 also altered the synaptic bouton marker, synaptophysin-ir, in a sex-specific manner, suggesting a role for PR activity in the development of perforant path innervation of the molecular layer (MOL). Finally, both control and RU486 treated rats spent significantly more time with a temporally distant object in the Relative Recency task, suggesting an intact associative memory for object identity and temporal order in both groups. In contrast, the same RU486 treated rats were impaired in an episodic-like memory task compared to controls, failing to integrate object identity (‘what’), time (‘when’), and object position (‘where’). These findings reveal a novel role for PR in regulating CR cell function within the MOL, thereby altering development of DG connectivity and behavioral function.

Keywords

Progesterone receptor; Cajal-Retzius; Perforant path; Dentate gyrus; Episodic memory; Reelin

*Corresponding author at: Department of Psychology, Social Science 399, University at Albany, 1400 Washington Ave., Albany, NY 12222, United States of America. cwagner@albany.edu (C.K. Wagner).

1. Introduction

Episodic memory, the ability to recollect specific episodes from one's past, is a fundamental component of human cognitive experience. Formally, episodic memory is defined as a declarative memory tied to the specific contextual and temporal cues of its acquisition (Tulving, 2002). The ability to accurately encode and recall these autobiographical memories provides the foundation for other complex human behaviors such as learning and planning for future events. Understanding the development of the neural substrates that mediate these behaviors, such as the hippocampus and its cortical connections, will provide a fuller understanding of the neurobiological basis of memory and cognition.

The hippocampus and the hippocampal circuit are critical for the formation and retrieval of episodic memory in humans (Eldridge et al., 2000; Scoville and Milner, 1957; Vargha-Khadem et al., 1997). In nonhuman primate and rodent models the hippocampus receives afferent input containing multimodal sensory details about the environment from cortical areas of the extended medial temporal lobe, particularly the entorhinal cortex (Agster and Burwell, 2013; Hevner and Kinney, 1996; Lavenex and Amaral, 2000; Witter, 2007; Witter et al., 2000). Behavioral studies in rodent models suggest that processing of sensory input in the entorhinal cortex is dissociated across different subregions. Specifically, the lateral entorhinal cortex (LEC) appears to regulate the processing of object identity, spatial context of objects, and egocentric spatial information, while the medial entorhinal cortex (MEC) appears to process head and body position within an environment, contextual information, and global spatial cues (Deshmukh and Knierim, 2011; Hafting et al., 2005; Hunsaker et al., 2007; Keene et al., 2016; Knierim et al., 2014; Kuruvilla and Ainge, 2017; Langston et al., 2010; Van Cauter et al., 2013; Wilson et al., 2013b, 2013a; Yoganarasimha et al., 2011).

The entorhinal cortex relays environmental sensory information to the dentate gyrus (DG) of the hippocampus via the fiber pathway known as the perforant path, which the DG then synthesizes into a conjunctive representation of the environment (Kesner, 2013; Morris et al., 2013), thereby representing an episodic memory of the what, where, when, and in which context an event occurred. The structure of this circuit makes the perforant path the primary conduit of episodic sensory information from the cortex to the hippocampal circuit, and positions the DG as a processing gateway to the rest of the hippocampus. These precise connections, which are established during critical windows of perinatal development, are integral to normal episodic memory. Therefore, it is critical to understand the mechanisms by which this pathway is formed during development and to identify the factors that guide its proper formation.

Development of synaptic connectivity between the perforant path and DG is established during the postnatal period. During the first postnatal week, entorhinal afferents arrive in the molecular layer (MOL) of the DG (Supèr et al., 1998; Tamamaki, 1999) and synaptogenesis between perforant path axons and granule cell dendrites begins soon after (Cowan et al., 1980; Duffy and Teyler, 1978, 1977; Rahimi and Claiborne, 2007). These processes are dependent on pioneer neurons of the DG MOL, known as Cajal-Retzius (CR) cells. CR cells form transient synapses with arriving perforant path axons (Supèr et al., 1998) and also regulate the normal innervation of the MOL by perforant path afferents (Borrell et al., 2007;

Del Río et al., 1997). Many CR cell functions rely on the synthesis and secretion of the glycoprotein, reelin. Insufficient reelin or over-expression of reelin both lead to abnormal synaptogenesis within the hippocampus (Bosch et al., 2016; Niu et al., 2008; Pujadas et al., 2010). Consequently, transcriptional changes in CR cells that might alter reelin expression would likely impact the integration of perforant path connectivity with the dentate gyrus (Del Río et al., 1997; Duveau et al., 2011).

We have previously reported that the nuclear steroid receptor, progesterone receptor (PR), is expressed in outer MOL CR cells of the rat DG during this critical epoch of postnatal development (Newell et al., 2018). Nuclear steroid receptors, such as PR, are widely expressed throughout the developing brain and, as transcription factors, can alter fundamental process of neural development. The regulation of gene expression in CR cells by PR (e.g., reelin expression) during neonatal life may be one mechanism by which normal development of perforant path connectivity is ensured. To test this hypothesis, following the pharmacological inhibition of PR activity during the first week of life, the number of reelin immunoreactive cells and the density of synaptophysin in the MOL DG was determined. Additionally, the effects of PR inhibition during development on subsequent episodic-like memory in adulthood were assessed.

2. Methods

2.1. Animals

All animal procedures were approved by the Institutional Animal Care and Use Committee at the University at Albany, SUNY and were in accordance with the 2011 Eighth Edition of the National Institute of Health Guide for the Care and Use of Laboratory Animals. Pregnant female rats were purchased from Taconic Laboratories (Germantown, NY) at approximately gestational day 15. Dams were housed singly in the same room, on a 12 hour light/dark cycle at a constant temperature of 25 ± 2 °C with food and water available ad libitum. Dams were allowed to deliver normally. Unless otherwise noted, pups were anaesthetized by hypothermia and euthanized via decapitation.

2.2. PR expression in dentate gyrus of males and females

Sex differences in adult hippocampal anatomy and function are well documented and are driven by steroid hormone receptor activity (Harburger et al., 2009; Leranth et al., 2004, 2003; Mukai et al., 2010; Woolley, 1998). However it is unknown if PR is expressed in rat DG at similar levels in males and females during development. To assess this potential sex difference, we performed immunohistochemistry for PR on male and female hippocampus at P7 and analyzed PR immunoreactivity in the infra and suprapyramidal MOL and SLM by light microscopy.

2.2.1. Tissue preparation—Rat pups were obtained from 5 litters, and each group contained at least three pups from each litter. On P7, male (N = 23) and female (N = 23) pups were anaesthetized by hypothermia and decapitated. Brains were removed and fixed for 6 h in 5% acrolein in 0.1 M phosphate buffered saline (PBS, pH 7.6) followed by 30% sucrose in 0.1 M PBS for 72 h. Serial coronal sections were taken through the extent of the

hippocampus on a freezing microtome at a thickness of 40 μm, and stored in cryoprotectant (30% sucrose, 0.1% polyvinylpyrrolidone-40, and 30% ethylene glycol in 0.1 M PB) at −20 °C until immunohistochemical processing.

2.2.2. Immunohistochemistry—Immunohistochemistry (IHC) was performed on free floating sections using the nickel enhanced 3′3-diaminobenzidine (DAB) peroxidase method to visualize PR-ir within the molecular layer of the dentate gyrus at P7. Briefly, sections were rinsed in 0.05 M Tris-buffered 0.9% saline (TBS) (3 × 5 min) to remove cryoprotectant solution, then incubated in 20% normal goat serum (NGS), 1% bovine serum albumin, and 1% hydrogen peroxide for 30 min. Sections were incubated in PR antisera made in rabbit (1:1000, DAKO Corp) in 0.5 M TBS, 2% NGS, and 0.3% Triton-X 100 for 48 h at 4 °C.

Sections were rinsed in 0.05 M TBS containing 1% NGS and 0.3% Triton-X 100 (TTG) (3 × 5 min). Sections were incubated with biotinylated goat anti-rabbit antibody, at a concentration of 5 μg/ml in TTG at R.T. for 90 min. Sections were then rinsed in TTG (2 × 5 min) and in 0.05 M TBS (2 × 5 min) before incubation with biotinylated horseradish peroxidase using the ABC Reagent kit (Vectastain Elite kit, Vector Laboratories) in 0.05 M TBS for 60 min. Sections were rinsed in 0.05 M TBS (3 × 5 min). Finally, sections were incubated in 0.05% 3′3 diaminobenzidine, 0.75 mM nickel ammonium sulfate, 0.15% β-D-glucose, 0.04% ammonium chloride, and 0.001% glucose oxidase in 0.05 M TBS until a dark brown/black reaction product was visible. Finally, sections were rinsed in 0.05 M TBS (5 × 5 min). Sections were mounted on gelatin-coated slides and dehydrated, delipidated, and cover slipped with Permount mounting reagent (Fisher Scientific, Pittsburg, PA).

2.2.3. Analysis of PR-ir—Three sections were selected from dorsal hippocampus from the rostral and middle extent of the hippocampus and anatomically matched across animals using one prenatal atlas and one adult atlas (Paxinos et al., 1994a, Figs. 168–171; Paxinos et al., 1994b, Figs. 32–35) by an experimenter blind to treatment. The total number of PR nuclei (dark brown or black-ir) across the entire extent of the infra and suprapyramidal blades of the DG were counted in each of the three sections and averaged. This process was repeated for both the rostral and middle sections respectively. Results were analyzed by a three way ANOVA (sex × region × subregion) ($p < 0.05$).

2.3. Role of PR activity in reelin and calretinin cell number

2.3.1. Tissue preparation—Male Rat pups were obtained from 4 litters. Approximately half of each litter was randomly assigned to the control group (N = 9) and half to the RU486 group (N = 13) to control for litter effects. Starting on the day of birth (postnatal day 1, P1), male pups were weighed and injected with the PR antagonist, RU486 (mifepristone, 20 mg/kg, s.c.) (N = 13), or an equal volume of the sesame oil vehicle alone (N = 9) daily through P7. On P7, pups were anaesthetized and intracardially perfused with 20–50 ml 0.9% saline (4 °C), followed by 4% paraformaldehyde in 0.1 M phosphate buffered saline (PBS, pH 7.6). Brains were removed and postfixed for 24 h in 4% paraformaldehyde in PBS. Brains were cryoprotected in 30% sucrose in 0.1 M PBS for 72 h. Serial coronal sections were taken through the extent of the hippocampus on a freezing microtome at a thickness of 40 μm, and stored in cryoprotectant (30% sucrose, 0.1% polyvinylpyrrolidone-40, and 30%

ethylene glycol in 0.1 M PB) were taken and stored at −20 °C until immunohistochemical processing.

2.3.2. Immunohistochemistry—Immunohistochemistry (IHC) was performed using the nickel enhanced 3′3-diaminobenzidine (DAB) peroxidase method as above, to visualize reelin-ir or calretinin-ir within the molecular layer of the dentate gyrus at P7. IHC was performed on two distinct series of separate sections, one series for reelin, one for calretinin, from each animal. Briefly, sections were rinsed in 0.05 M Tris-buffered 0.9% saline (TBS) (3 × 5 min) to remove cryoprotectant solution, then incubated in 20% normal goat serum (NGS) for reelin or normal horse serum (NHS) for calretinin, 1% bovine serum albumin, and 1% hydrogen peroxide for 30 min. Sections were incubated in anti-reelin primary antibody made in mouse (1:1000, MAB5366, Millipore, Temecula CA) or anti-calretinin primary antisera made in goat (1:1000, AB1550, Millipore, Temecula CA) in 0.5 M TBS, 2% NGS, and 0.3% Triton-X 100 for 48 h at 4 °C.

Sections were rinsed in 0.05 M TBS containing 1% NGS and 0.3% Triton-X 100 (TTG) (3 × 5 min). Sections were then incubated in biotinylated goat anti-mouse antibody for reelin and, biotinylated mouse anti-goat raised mouse for calretinin, at a concentration of 5 μg/ml in TTG at R.T. for 90 min. Sections were then rinsed in TTG (2 × 5 min) and in 0.05 M TBS (2 × 5 min) before incubation with biotinylated horseradish peroxidase using the ABC Reagent kit (Vectastain Elite kit, Vector Laboratories) in 0.05 M TBS for 60 min. Sections were rinsed in 0.05 M TBS (3 × 5 min). Finally, sections were incubated in 0.05% 3′3 diaminobenzidine, 0.75 mM nickel ammonium sulfate, 0.15% β-D-glucose, 0.04% ammonium chloride, and 0.001% glucose oxidase in 0.05 M TBS until a dark brown/black reaction product was visible (reelin 5:30 mins, calretinin 6:30 mins). Sections were rinsed in 0.05 M TBS (5 × 5 min). Sections were mounted on gelatin-coated slides and dehydrated, delipidated, and cover slipped with Permount mounting reagent (Fisher Scientific, Pittsburg, PA).

2.3.3. Analysis of reelin-ir/calretinin-ir—Analysis of reelin-ir sections and calretinin-ir sections was conducted in separate, but parallel analyses. In both cases, three sections from dorsal hippocampus were selected and anatomically matched across animals with use of a prenatal (Paxinos et al., 1994b, Figs. 166–170) and an adult brain atlas (Paxinos and Watson, 1998, Figs. 32–35) by an experimenter blind to treatment group. The total number of cells positive for reelin or calretinin immunoreactivity was counted unilaterally in all three sections at 20× throughout the entire medio-lateral extent of the suprapyramidal blade of the MOL, and within the stratum lacunosum moleculare. For each animal, the number of immunoreactive cells per section was averaged across the three dorsal sections to create a mean cell number for each animal. Results for reelin and calretinin were analyzed separately by one way analysis of variance (ANOVA) with treatment as the independent variable and mean number immunoreactive cells as the dependent variable. Eta Squared (η^2) was calculated for significant main effects and interactions to determine effect size.

2.4. Role of PR activity on P7 MOL synaptic boutons

The first postnatal week is an important period in the development of perforant path/DG connectivity and coincides with the height of PR expression in CR cells of the MOL. From (P0–5) axons of the entorhinal cortex synapse on calretinin expressing cells in the MOL, putatively CR cells (Supèr et al., 1998). By P7, granule cell dendrites are still extending into the MOL and only a small proportion exhibit dendritic spines, suggesting they are functionally immature and have not yet made synapses with entorhinal afferents (Jones et al., 2003; Tamamaki, 1999). Therefore, this early postnatal period ending by P7, represents an initial stage in perforant path/DG synaptic ontogeny, at which time afferents have arrived and made synapses with CR cells, but have yet to establish long term connections with granule cells, their final targets. To assess the role of PR activity on the extent of synapse formation in the MOL during this early postnatal period, we analyzed the area of synaptophysin immunoreactivity in the MOL of RU486 or/Oil treated rats at P7.

2.4.1. Tissue preparation & immunocytochemistry—Rat pups were obtained from 12 litters. Approximately half of each litter were randomly assigned to the P7 study, and of those half were randomly assigned to the control group (N = 33, 17 males, 16 females), and half to the RU486 group (N = 34, 16 males, 18 females) to control for litter effects. Approximately half of the rats pups from the 12 litters were utilized (the other half being used at P21) for a total of 67 animals. Rat pups were treated with RU486 or vehicle from P1 to P7 as describe above. Brains from males and females were collected at P7 as described above. Immunohistochemistry was performed for synaptophysin as detailed above. Briefly, sections were incubated with anti-synaptophysin primary antibody made in mouse (1:5000; S5768, Sigma, St. Louis, MO) in TTG for 48 h at 4 °C, then in biotinylated goat anti-mouse antibody in TTG for 90 min at R.T., followed by ABC reagent for 60 min in 0.05 M TBS. Sections were then incubated (6 min) in 0.05% 3′3 diaminobenzidine, 0.75 mM nickel ammonium sulfate, 0.15% β-D-glucose, 0.04% ammonium chloride, and 0.00025% glucose oxidase in 0.05 M TBS and thoroughly rinsed in 0.05 M TBS before mounting and coverslipping as described above.

2.4.2. Synaptophysin-ir analysis—An anatomically matched section within the dorsal hippocampus, was chosen for each animal with use of a stereotaxic atlas (Paxinos et al., 1994b, Fig. 170) by an experimenter blind to treatment group as described above. Photomicrographs were taken at 20× in the unilateral suprapyramidal and infrapyramidal blades of the dentate gyrus. Image processing and analysis for P7 tissue was performed in Scion image. The total area (μm^2) covered by thresholded pixels (representing specific synaptophysin-ir above background) was analyzed within the suprapyramidal blade and the infrapyramidal blade of the DG was analyzed. Results were analyzed by a three way ANOVA (sex × treatment × region) and significant interactions were further analyzed using two way ANOVAs with factors of treatment and sex within each region. η^2 was calculated for significant main effects and interactions to determine effect size. Pre-planned, multiple comparisons were made using the Student-Newman-Keuls test ($p < 0.05$), and effect size was calculated as Cohen's d.

2.5. Role of PR activity in P21 MOL synaptic density

Postnatal days P10–21 represents a period of intense synaptogenesis in the DG. During this time the number of synapses in the MOL increases by 3–5 fold (Cowan et al., 1980), concurrent with an increase in complexity of the granule cell dendritic plexus and maturation of granule cell dendritic spines (Jones et al., 2003). Also observable at P14, a process of synaptic remodeling begins, ostensibly refining dentate/entorhinal synapses and establishing adult-like connections (Rahimi and Claiborne, 2007). P21 therefore, represents a subsequent second phase of perforant path/DG maturation to P7, a period of both synaptic elaboration and refinement that prepares the way for adult hippocampal connectivity. If the initial conditions of MOL synapse development are altered by PR activity at P7, these changes may ripple forward to subsequently impact the state of MOL synaptogenesis at P21.

2.5.1. Tissue preparation—Rat pups were obtained from 12 litters. Approximately half of each litter was randomly assigned to the control group (N = 32, 17 males, 15 females), and half to the RU486 group (N = 33, 15 males, 18 females) to control for litter effects. Half the rat pups from the 12 litters were utilized (the other half being used at P7) for a total of 65 animals. Pups were treated with RU486 or vehicle from P1 to P7 as describe above. At P21, male and female rats were deeply anaesthetized with a lethal dose of sodium pentobarbital (i.p.) and intracardially perfused with 30–50 ml 0.9% saline (4 °C), then 4% paraformaldehyde in 0.1 M PBS (4 °C). Brains were removed, postfixed in 4% paraformaldehyde in 0.1 M PBS for 24 h, and cryoprotected as described above prior to sectioning.

2.5.2. Synaptophysin-ir analysis—Due to the much larger size of the hippocampus at P21, two sections from each animal were analyzed across the rostro-caudal extent of the structure. A section from the rostral portion of the dorsal hippocampus (‘Rostral’ corresponding to Fig. 32 in Paxinos and Watson, 1998), and a section from a more caudal region of the dorsal hippocampus (‘Middle’ corresponding to Fig. 35 in Paxinos and Watson, 1998), were selected and anatomically matched across animals by an experimenter blind to treatment group. Photomicrographs were taken at 100× unilaterally in the suprapyramidal and infrapyramidal blades of the dentate gyrus. Given the significant qualitative differences in synaptophysin immunoreactivity observed in the dentate gyrus at P7 (diffuse) and P21 (punctate), different methods of analysis were utilized for the two ages. Image processing and analysis of P21 tissue was performed in Image J.

For each P21 image, nonspecific background was systematically removed from all images using a consistent criteria (Image J function Subtract Background), and the image was converted to binary. This process consistently rendered non-specific background white, and specific synaptophysin-ir puncta black. Two representative regions of constant area (450 μm^2) were selected within the infrapyramidal and suprapyramidal blades and the area covered by black pixels calculated (representing specific synaptophysin-ir). Total synaptophysin-ir was averaged across the two selected 21.21 × 21.21 μm areas to create a single measure for each blade in each animal. Results were analyzed using a three way ANOVA (sex × treatment × region). Since no significant three -way interaction was observed, two-way ANOVAs were not performed (as at P7), η^2 was calculated for

significant main determine effect size. Pre-planned, multiple group comparisons were made using the Student-Newman-Keuls test ($p < 0.05$) and effect size was calculated for group comparisons as Cohen's d.

2.6. Behavioral testing

2.6.1. Animals—Animals used for behavioral testing were obtained from 8 litters. Half of each litter was randomly assigned to the control group, and half to the RU486 group to control for litter effects. All of the male pups from the 8 litters were utilized for a total of 46 animals, half treated with RU486 (N = 23) and half vehicle (N = 23) from P1 to P7. Pups were housed as described above until P21. At P21, male rats were weaned and housed two per cage until habituation began at P60. The same animals were utilized in first the Episodic-like memory task and then the Relative Recency task. There was no overlap in objects used in the Episodic-like memory task and the Relative Recency task. At P60, male rats were transported to the behavioral suite where testing was to take place, removed from their home cage, and handled by two experimenters for 3 min each. Following handling, each rat was placed in the open field apparatus (70 cm × 70 cm × 40 cm) used for both behavior tasks. During habituation to the apparatus two sample testing objects (objects similar to, but not identical to, objects used during testing) and allowed to explore for 3 min. This habituation occurred daily for 14 days.

2.6.2. The role of postnatal PR activity on the Relative Recency task—All behavioral task test sessions were recorded by a webcam positioned directly over the open field arena and saved on a computer with coded file names for experimenter analysis. The Relative Recency task uses two sets of different stimulus objects presented during separate trials to test specifically, the "what" and "when" components of episodic-like memory. In Sample 1, the animal is presented with two identical objects and allowed to explore for 5 min (Fig. 1). Following a 50 min intertrial interval (ITI), in Sample 2, the animal is presented with a different set of two identical objects for 5 min. Following a 50 min ITI, in Test trial, the animal is presented with one object from Sample 1 (distant) and one object from Sample 2 (recent) and allowed to explore for 5 min. Differential exploration time with each object (distant versus recent) in the test phase reflects the animals' ability to distinguish between the objects and when each object was seen, or a memory for "what" (object identity, i.e. red star or blue circle in Fig. 1) and "when" the object was seen (distant versus recent, Sample 1 versus Sample 2).

2.6.3. The role of postnatal PR activity on the Episodic-like Memory task—The episodic-like memory task tests animals' ability to integrate three components of episodic-like memory: "what" "when" and "where". In Sample 1, four identical objects are presented for 5 min in an open field arena (distant) (Fig. 2). Following a 50 min ITI, in Sample 2, a different set of four identical objects are presented in the arena (recent). Following a 50 min ITI, in the Test trial, two objects from Sample 1 and two objects from Sample 2 are presented together for 5 min. One of the objects of each set remains stationary, in the same location it was previously presented in the Sample (stationary), while the other object is moved to a new location (displaced). This arrangement creates four objects which vary on three components of episodic-like memory, object identity ('what', green square

versus purple triangle), temporal order of experience ('when', distant versus recent), and object location ('where', stationary versus displaced). Differential object exploration reflects the rat's ability to remember a combined representation, or an integration, of what object was seen when and where.

2.6.4. Analysis of behavioral tasks—For both Relative Recency and Episodic-Like Memory tasks, recorded test sessions were scored by two experimenters blind to treatment group for time (s) spent exploring objects. Object exploration was defined as sniffing, whisking, licking, or looking at an object from less than 1 cm away. Total object exploration time, as well as exploration time per individual object were averaged between the two experimenters. Results for the Relative Recency task were analyzed by two way repeated measure ANOVA (treatment × when). To analyze each groups' ability to integrate all three components of episodic-like memory, results for the ELM task were analyzed by separate two way ANOVAs (when × where) for each treatment group (Oil and RU486) as previously reported (Barbosa et al., 2012), η^2 was calculated for significant main effects to determine effect size. Pre-planned post hoc comparisons were made using Fisher's Least Significant Difference test ($p < 0.05$), and effect size was calculated as Cohen's d.

3. Results

3.1. PR expression in the DG is similar in males and females at P7

The mean number of PR immunoreactive cells (PR-ir) in the rostral and middle dorsal DG was similar in males and females. Three way ANOVA (sex × region × subregion) demonstrated there was no significant main effect of sex and significant interaction of sex and region, sex and subregion, and no significant three way interaction (Fig. 3).

3.2. Inhibition of PR during development increases reelin-ir, but not calretinin-ir, cell number in DG MOL

The mean number of reelin-ir cells in the MOL of the DG was significantly higher in RU486 treated rats compared to controls at P7 (Fig. 4). One way ANOVA revealed a significant main effect of treatment ($F_{1, 1} = 14.46$, $p = 0.001$, $\eta^2 = 0.46$).

To determine whether the observed change in the number of reelin-ir cells could be attributed to an actual increase in the number of CR cells or to a change in levels of reelin within CR cells, the number of calretinin-ir cells (another marker of CR cells in the MOL (Anstötz and Maccaferri, 2020)) was counted in alternate sections. The number of calretinin-ir cells was not significantly different in rats treated with RU486 compared to control animals ($F_{1, 1} = 1.466$, $p = 0.241$) (Fig. 4), suggesting the effect of RU486 may not change CR cell number, but instead reelin levels. There was a similar number of calretinin-ir and reelin-ir cells in control animals.

3.3. Inhibition of PR during development alters synaptophysin-ir density in MOL DG at P7

Three-way ANOVA revealed a significant three-way interaction (Sex × Treatment × Region; $F_{1,99} = 5.037$ $p < 0.05$, $\eta^2 = 0.27$) and a significant two way interaction between sex and treatment ($F_{1,99} = 4.250$ $p < 0.05$, $\eta^2 = 0.23$), but no significant interaction between

treatment and region, or sex and region. Additionally, there was no main effect of sex or treatment (Fig. 5). Because the three-way ANOVA indicated differential effects of RU486 depending on region of the MOL, we analyzed the infrapyramidal and suprapyramidal blades independently with separate two way ANOVAs.

In the infrapyramidal blade of the DG, there was a trend suggesting that RU486 treated rats exhibited a higher mean area of synaptophysin-ir in the MOL than oil controls (main effect of treatment $p = 0.06$, $\eta^2 = 0.07$; Fig. 5A).There was no significant main effect of sex and no significant interaction of sex and treatment. In the suprapyramidal blade of the DG, two-way ANOVA demonstrated a significant interaction (Sex × Treatment, $F_{1, 49} = 8.581$, $p = 0.005$; $\eta^2 = 0.15$, Fig. 5B) but no significant main effect of sex or treatment. Posthoc analyses revealed a significant difference between control males and females ($p = 0.012$, $d = 0.20$; Fig. 5B) in area of synaptophysin-ir in the suprapyramidal blade. Additionally, RU486 treatment significantly increased synaptophysin-ir in the MOL of males ($p = 0.017$, $d = 0.18$; Fig. 5B) but not in females, thereby abolishing the sex difference.

3.4. Inhibition of PR during development alters synaptophysin-ir density in MOL at P21

Sections from the rostral and middle hippocampus were analyzed separately for density of synaptophysin-ir in the infrapyramidal and suprapyramidal blades of the MOL in P21 male and female rats. In rostral hippocampus, three-way ANOVA revealed a significant two-way interaction (sex × treatment, $F_{1, 53} = 5.344$, $p = 0.025$, $\eta^2 = 0.08$; Fig. 6A), but no significant three-way interaction and no significant interaction between sex and region, or treatment and region. Additionally, there were no significant main effects of sex or treatment. Post hoc pairwise comparison revealed a significant difference between RU486 treated males and RU486 treated females ($p = 0.011$, $d = 0.66$), but there was no significant sex difference in control animals.

In the middle hippocampus, three-way ANOVA revealed a significant two-way interaction (sex × treatment, $F_{1, 119} = 3.943$, $p = 0.049$, $\eta^2 = 0.03$; Fig. 6B), but no significant three way interaction and no significant interaction between sex and region, or treatment and region. Additionally there were no significant main effects of sex or treatment. Post hoc pairwise comparison revealed a significant effect of RU486 in females (treatment within female, $p = 0.034$, $d = 0.11$; Fig. 6B) and no significant effect of RU486 in males.

3.5. Inhibition of PR impairs integration of ELM but not specific ‘what’, ‘when’ components

In the Relative Recency task there was no significant effect of RU486 treatment in the total time exploring all objects ($p = 0.49$, Fig. 7) suggesting similar motivation to explore objects in both groups. Two-way repeated measures ANOVA revealed a main effect of ‘when’ ($F_{1, 44} = 10.905$, $p = 0.002$, $\eta^2 = 0.20$; Fig. 7), but no significant main effect of treatment and no significant interaction between treatment and ‘when’. Post hoc comparisons revealed a trend that oil treated animals spent significantly more time with the ‘distant’ object compared with the ‘recent’ object ($p = 0.051$, $d = 0.15$; Fig. 7) and RU486 treated animals spent significantly more time exploring the ‘distant’ object compared to the ‘recent’ object ($p = 0.011$, $d = 0.30$; Fig. 7).

In the ELM task, analysis of the control group by repeated measures two way ANOVA showed there was no significant difference in the total time exploring the objects as a whole between the two groups in the test session ($p = 0.30$) (Fig. 8), suggesting no difference between the groups in motivation to explore the objects. Two-way repeated measures ANOVA within the control group demonstrated a significant main effect of 'where' ($F_{1, 21} = 6.155$, $p = 0.021$, $\eta^2 = 0.08$; Fig. 8A). However, there was no significant main effect of 'when' and no significant interaction between 'where' and 'when'. Post hoc pairwise comparisons revealed that control animals spent significantly more time interacting with the distant stationary object compared to the distant displaced object ($p = 0.032$; $d = 0.11$; Fig. 8A), while there was no significant difference in time spent exploring the recently presented objects whether they were stationary or displaced. The preference of the control group to explore the 'distant stationary' over object compared to the 'distant displaced' object suggests that these animals were capable of recalling 'what' object they observed 'when' and 'where' and stands in contrast to the RU486 treated group which showed no such preference. Two-way repeated measure ANOVA revealed no significant main effect of 'when' or 'where' and no significant interaction between 'when' and 'where' in the RU486 treated rats (Fig. 8B).

4. Discussion

The nuclear steroid receptor, progesterone receptor, is transiently expressed in Cajal-Retzius cells of the DG MOL during the postnatal period (Newell et al., 2018). CR cells synthesize and secrete the glycoprotein, reelin, which is integral to the normal development of granule cell innervation by arriving perforant path axons (Del Río et al., 1997; Supèr et al., 1998). Over-expression of reelin increases, and reelin knockout decreases, synaptic contacts in the DG (Bosch et al., 2016; Niu et al., 2008; Pujadas et al., 2010). Findings from the present study demonstrate that inhibition of PR activity with the antagonist, RU486, during the first week of life increased the number of reelin-ir cells in the MOL at P7 compared to controls. Additionally, treatment with RU486 increased synaptophysin-ir, a marker of synaptic boutons, within the MOL (Calhoun et al., 1996; Mouton et al., 1997). There was a novel sex difference in the total amount of synaptophysin-ir in the suprapyramidal MOL of control rats on P7 (females > males), representing one of the first reported sex differences in developing DG. Interestingly, the sex difference was abolished by RU486 treatment. PR inhibition from P1 to 7 also exerted long lasting effects in MOL. Postnatal RU486 treatment had differential effects on males and females in rostral infrapyramidal MOL, increasing the density of synaptophysin-ir in females, but decreasing it in males. In middle MOL, RU486 treatment induced a sex difference in synaptophysin-ir that was not present in controls. These findings suggest that PR activity during the first postnatal week is critical for the normal development of afferent input to the dentate gyrus and may do so in a sex-specific manner.

Inhibition of PR activity during development disrupted episodic-like memory, but not two-component associative memory in adulthood. In the RR task, RU486 treated rats were able to remember 'what' and 'when' as well as controls. The disruption of behavior arose in the ELM task which added the spatial component of 'where,' suggesting that inhibition of PR during development specifically perturbed the ability to integrate all three components into

an intact episodic memory, an ability theorized to rely on DG processing of sensory information (Hunsaker et al., 2007; Kesner, 2018, 2013).

4.1. Inhibition of PR alters MOL reelin at P7

PR expression in CR cells, which peaks between birth and P7, but continues over the first three weeks of life (Newell et al., 2018), temporally coincides with the innervation of the MOL by entorhinal afferents, that occurs from about P1 through P11 (Borrell et al., 2007; Supèr et al., 1998; Tamamaki, 1999). This innervation of the MOL is dependent on the secretion of reelin from CR cells and indeed, inhibition of PR from P1 to 7 significantly increased the number of reelin-ir cells in the MOL of rats at P7. Reelin is a critical signaling molecule in the process of lamina-specific innervation of the DG by entorhinal afferents. For example, treatment of organotypical slice cultures with anti-reelin antibody caused perforant path fibers to overshoot their target lamina (MOL) and grow ectopically into other regions of the DG (Del Río et al., 1997). This process is likely mediated by the interaction of extracellular reelin, secreted by CR cells, with axonal growth cones of entorhinal axons that express dab1, an adaptor protein of the reelin molecular cascade (Borrell et al., 2007). The increase in reelin-ir following PR inhibition suggests that PR activity may be critical for normal reelin-regulated perforant path innervation of the MOL.

In addition to reelin, CR cells also express calretinin protein (Anstötz et al., 2018). In the present study, there was no difference in the number of reelin-ir and calretinin-ir CR cells in controls rats. While RU486 increased the number of CR cells detected by reelin-ir, there was no change in the number of CR cells containing calretinin-ir in the same animals. This suggests that the increase in reelin-ir cell number can most likely be attributed to an increase in the levels of intracellular reelin protein within CR cells, as opposed to an actual increase in the number of CR cells.

Although it is possible that the reelin and calretinin immunoreactive cells quantified are not the same population of CR cells, this seems unlikely given several factors. First, the morphology of cells counted in both the calretinin and reelin study share the same distinctive ‘tadpole’ like morphology of CR cells, and same small ovoid somal size (Fig. 4A, 4B) suggesting they are the same cell type. Second, recent research has demonstrated that the vast majority (82.4%) of calretinin expressing cells in the entire MOL of the P7 DG are CR cells, and indeed this proportion increases when looking specifically at the outer MOL, where CR cells are the overwhelming majority cell type (Anstötz and Maccaferri, 2020). Indeed the outer MOL is the same anatomical region quantified in this study. Together, this suggests that reelin-ir and calretinin-ir cells of the outer MOL are likely the same population of CR cells.

High intracellular reelin levels could result from increased transcription of reelin protein or from decreased secretion of reelin, both of which would presumably impact MOL synaptogenesis. Indeed, over-expression of reelin in mice results in dendritic hypertrophy, larger synapses, increased granule cell mushroom spines, as well as increased density of synapses in the MOL (Bosch et al., 2016; Pujadas et al., 2010). In contrast, reelin genetic knockout resulted in changes to hippocampal pre and postsynaptic elements, including decreased collateralization, branching and extension of entorhinal axons (Borrell et al.,

1999) as well as reduced dendritic spine density (Niu et al., 2008). Therefore, whether PR activity induces increased or decreased extracellular reelin, it likely has a critical impact on the formation of MOL synapses. There is a paucity of research about the genomic ensemble regulated by PR in non-neuroendocrine regions of the brain, such as the hippocampus and cortex, making it potentially difficult to propose a regulatory mechanism between PR and reelin until further research is done.

4.2. Inhibition of PR alters synaptic boutons across DG development

Inhibition of PR during the postnatal period had both acute and long lasting effects on the area and density of synaptic boutons in the MOL. Treatment with RU486 from P1 to P7 significantly increased the amount of synaptophysin-ir at P7 in the suprapyramidal MOL of male rats, abolishing the novel sex difference observed in controls. At P21, there was no sex difference in synaptic bouton density in controls. However, RU486 had differential and persistent sex-dependent effects on MOL synaptic boutons at P21. In both the rostral and middle hippocampus, RU486 treated females had significantly higher density of synaptophysin-ir, particularly in the infra pyramidal MOL, compared to RU486 treated males.

These changes in synaptic boutons occur against the backdrop of a dynamic synaptic ontogeny between entorhinal afferents and cells of the DG during the first three postnatal weeks in the MOL. At P7, initial innervation of the MOL by entorhinal axons has occurred, and temporary synapses with CR cells have formed (Deng et al., 2006; Supèr et al., 1998; Tamamaki, 1999). This represents an immature stage before entorhinal axons have formed synapses with granule cells (Rahimi and Claiborne, 2007). Therefore, the increased synaptophysin-ir at P7 may represent an increase in transient perforant path/CR synapses. In contrast to the first postnatal week, by P21 granule cell dendrites are morphologically and physiologically mature, and the total number of synapses in the MOL has greatly increased (Cowan et al., 1980; Duffy and Teyler, 1978; Rahimi and Claiborne, 2007), thereby representing a more mature stage of MOL connectivity. The increase in the density of synaptophysin-ir by postnatal RU486 in females, but not males, in rostral and middle DG suggests an increased innervation of granule cell dendrites by entorhinal cortex afferents, and that neonatal PR activity may exert effects on perforant path function later in life.

4.3. Inhibition of PR activity influences adult episodic-like memory

Inhibition of PR during the first postnatal week impaired the ability to integrate the components of episodic-like memory in adult rats. Control rats spent significantly more time exploring the ‘distant stationary’ object when compared to the ‘distant displaced’ object, a typical finding of the ELM paradigm (Dere et al., 2005; Kart-Teke et al., 2006; Rossetti et al., 2017). This suggests that control rats differentiate the objects on the basis of both place (stationary vs displaced) and time (they show this preference specifically in the case of the distant objects). In other words, control rats have an integrated memory for ‘when’ they encountered the objects (distant vs recent), and can differentiate the objects from each other based on ‘where’ they were located in the sample phase (stationary vs displaced). However, rats treated with RU486 spent a similar amount of time with all stimulus objects, suggesting

that these animals were unable to differentiate between ‘what’ object was seen, and ‘when’ or ‘where’ it was encountered, suggesting a significant impairment of ELM.

Importantly, the memory deficits in RU486 rats were specific to the integration of ‘what’, ‘where’, and ‘when’, and were not simply an impairment of associative memory in general. This fact is illustrated by the results of the RR Task. In the RR Task, the same RU486 treated rats demonstrated intact associative memory for ‘what object’ was seen ‘when’, spending significantly more time exploring the temporally distant object compared to the more recently presented object.

The PR antagonist RU486 also has affinity for the glucocorticoid receptor (GR), because of this, effects of GR activity on the present results cannot be ruled out. However, there are several reasons why this alternative is unlikely. Treatment with RU486 during the first postnatal week overlaps with the postnatal stress hyporesponsive period in the rat, a period during the first two postnatal weeks characterized by exceptionally low levels of circulating stress hormones (Henning, 2020; Meaney et al., 1985; Sapolsky and Meaney, 1986). Given this, during this postnatal stress hyporesponsive period normal stressors do not evoke corticosterone release from the adrenals (Cote and Yasumura, 1975). Second, GR protein and mRNA levels are very low in the DG for the first 10 postnatal days with most extant GR expression confined to granule cells (Galeeva et al., 2010, 2006). Finally, RU486 treated animals and controls had a similar number of central grid crossings and amount of time they spent in the central portion of the testing arena in an open field test, two behavioral measures of anxiety (Newell et al., 2018). If GR activity was disrupted during the postnatal period, its effect might be reflected in altered behavioral indicators of anxiety, however this was not observed.

It is possible that postnatal injection of pups might elicit some behavioral change that could manifest in adulthood, however the absence of typical stress response also suggests that any effect of stress created by injection during the first postnatal week is likely blunted. Indeed in a previous study, rat pups injected with oil vehicle for the first 10 postnatal days, showed no significant difference in anxiety behavior on the elevated plus maze task when compared to un-injected controls (Lonstein et al., 2001), suggesting postnatal injection may not alter stress related behaviors in adulthood.

Taken together, these findings demonstrate that RU486 treated rats can readily recall sensory components of an experience, representing object identity and episodic time in the RR task, yet these same animals fail to distinguish object identity or episodic time when asked to integrate these three components into an episodic memory, a process thought to be dependent on the DG (in the ELM task). Integration of sensory components (such as object identity and spatial components) is theorized to require the DG for synthesis of ELM (Hunsaker et al., 2007; Kesner and Rolls, 2015; Morris et al., 2013). If DG innervation is altered during development, perhaps through changes in reelin or CR cell function driven by PR inhibition, we might expect to see deficits in behaviors requiring integration of sensory components, such as the formation of ELM.

5. Conclusion

The present study reveals a potential role for PR, a powerful transcription factor, in the development of normal DG connectivity and formation of circuitry underlying episodic memory. PR activity during a fundamental developmental stage of DG synaptic connectivity, appears to maintain intracellular reelin within CR cells, either through changes in reelin expression or secretion. This regulation of extracellular reelin levels may ensure normal CR-dependent connectivity between afferents arriving from entorhinal cortex and granule cell dendrites in the MOL. PR activity during development also appears to be necessary for the integration of the what, where and when components of memory, the hallmark of episodic memory. These findings implicate PR as an important regulator of pioneer cell function and extend our knowledge about the factors that regulate development of hippocampal circuitry that underlies complex memory formation in adulthood.

Acknowledgments

Supported by National Institue of Child Health and Human Develpment (USA) HD076430 and HD093907 to CKW.

References

Agster KL, Burwell RD, 2013. Hippocampal and subicular efferents and afferents of the perirhinal, postrhinal, and entorhinal cortices of the rat. Behav. Brain Res 254, 50–64. doi:10.1016/j.bbr.2013.07.005. [PubMed: 23872326]

Anstötz M, Maccaferri G, 2020. A toolbox of criteria for distinguishing Cajal–Retzius cells from other neuronal types in the postnatal mouse hippocampus. eNeuro 7.

Anstötz M, Quattrocolo G, Maccaferri G, 2018. Cajal-Retzius cells and GABAergic interneurons of the developing hippocampus: close electrophysiological encounters of the third kind. Brain Res 1697, 124–133. 10.1016/j.brainres.2018.07.028. [PubMed: 30071194]

Barbosa FF, de Oliveira Pontes IM, Ribeiro S, Ribeiro AM, Silva RH, 2012. Differential roles of the dorsal hippocampal regions in the acquisition of spatial and temporal aspects of episodic-like memory. Behav. Brain Res 232, 269–277. 10.1016/j.bbr.2012.04.022. [PubMed: 22546523]

Borrell V, Del Río J. a, Alcántara S, Derer M, Martínez A, D'Arcangelo G, Nakajima K, Mikoshiba K, Derer P, Curran T, Soriano E, 1999. Reelin regulates the development and synaptogenesis of the layer-specific entorhino-hippocampal connections. J. Neurosci 19, 1345–1358 (doi:citeulike-article-id:179771). [PubMed: 9952412]

Borrell V, Pujadas L, Simo S, Dura D, Sole M, Cooper JA, Del Rio JA, Soriano E, 2007. Reelin and mDab1 regulate the development of hippocampal connections. Mol. Cell. Neurosci 36, 158–173. 10.1016/j.mcn.2007.06.006. [PubMed: 17720534]

Bosch C, Masachs N, Exposito-Alonso D, Martínez A, Teixeira CM, Fernaud I, Pujadas L, Ulloa F, Comella JX, Defelipe J, Merchán-Ṕrez A, Soriano E, 2016. Reelin regulates the maturation of dendritic spines, synaptogenesis and glial ensheathment of newborn granule cells. Cereb. Cortex 26, 4282–4298. 10.1093/cercor/bhw216. [PubMed: 27624722]

Calhoun ME, Jucker M, Martin LJ, Thinakaran G, Price DL, Mouton PR, 1996. Comparative evaluation of synaptophysin-based methods for quantification of synapses. J. Neurocytol 25, 821–828. 10.1007/s00330-011-2364-3. [PubMed: 9023727]

Cote TE, Yasumura S, 1975. Effect of ACTH and histamine stress on serum corticosterone and adrenal cyclic AMP. Endocrinology 96, 1044–1047. [PubMed: 164340]

Cowan WM, Stanfield BB, Kishi K, 1980. The development of the dentate gyrus. Curr. Top. Dev. Biol 30, 103–157.

Del Río J. a, Heimrich B, Borrell V, Förster E, Drakew A, Alcántara S, Nakajima K, Miyata T, Ogawa M, Mikoshiba K, Derer P, Frotscher M, Soriano E, 1997. A role for Cajal-Retzius cells and reelin

in the development of hippocampal connections. Nature 385, 70–74. 10.1038/385070a0. [PubMed: 8985248]

Deng J. do, Yu DM, Li MS, 2006. Formation of the entorhino-hippocampal pathway: a tracing study in vitro and in vivo. Neurosci. Bull 22, 305–314. 10.1680/udap.2010.163. [PubMed: 17690715]

Dere E, Huston JP, De Souza Silva MA, 2005. Episodic-like memory in mice: simultaneous assessment of object, place and temporal order memory. Brain Res. Protocol 16, 10–19. 10.1016/j.brainresprot.2005.08.001.

Deshmukh SS, Knierim JJ, 2011. Representation of non-spatial and spatial information in the lateral entorhinal cortex. Front. Behav. Neurosci 5, 1–33. 10.3389/fnbeh.2011.00069. [PubMed: 21267359]

Duffy CJ, Teyler TJ, 1977. Development of habituation in the dentate gyrus of rat: physiology and anatomy. Brain Res. Bull 3, 305–310.

Duffy CJ, Teyler TJ, 1978. Development of potentiation in the dentate gyrus of rat: physiology and anatomy. Brain Res. Bull 3, 425–430. [PubMed: 122707]

Duveau V, Madhusudan A, Caleo M, Knuesel I, Fritschy J-M, 2011. Impaired reelin processing and secretion by Cajal-Retzius cells contributes to granule cell dispersion in a mouse model of temporal lobe epilepsy. Hippocampus 21, 935–944. 10.1002/hipo.20793. [PubMed: 20865728]

Eldridge LL, Knowlton BJ, Furmanski CS, Bookheimer SY, Engel SA, 2000. Remembering episodes: a selective role for the hippocampus during retrieval. Nat. Neurosci 3, 1149–1152. [PubMed: 11036273]

Galeeva A, Ordyan N, Pivina S, Pelto-Huikko M, 2006. Expression of glucocorticoid receptors in the hippocampal region of the rat brain during postnatal development. J. Chem. Neuroanat 31, 216–225. 10.1016/j.jchemneu.2006.01.004. [PubMed: 16533592]

Galeeva A, Pelto-Huikko M, Pivina S, Ordyan N, 2010. Hormones of the limbic system postnatal ontogeny of the glucocorticoid receptor in the hippocampus. Vitam. Horm 10.1680/udap.2010.163.

Hafting T, Fyhn M, Molden S, Moser M, Moser EI, 2005. Microstructure of a spatial map in the entorhinal cortex. Nature 436, 801–806. 10.1038/nature03721. [PubMed: 15965463]

Harburger LL, Saadi A, Frick KM, 2009. Dose-dependent effects of post-training estradiol plus progesterone treatment on object memory consolidation and hippocampal extracellular signal-regulated kinase activation in young ovariectomized mice. Neuroscience 160, 6–12. 10.1016/j.neuroscience.2009.02.024. [PubMed: 19223011]

Henning SJ, 2020. Plasma Concentrations Corticosterone During of Total and Free Development in the Rat

Hevner RF, Kinney HC, 1996. Reciprocal entorhinal-hippocampal connections established by human fetal midgestation. J. Comp. Neurol 372, 384–394. [PubMed: 8873867]

Hunsaker MR, Mooy GG, Swift JS, Kesner RP, 2007. Dissociations of the medial and lateral perforant path projections into dorsal DG, CA3, and CA1 for spatial and nonspatial (visual object) information processing. Behav. Neurosci 121, 742–750. 10.1037/0735-7044.121.4.742. [PubMed: 17663599]

Jones SP, Rahimi O, Boyle MPO, Diaz DL, Claiborne BJ, 2003. Maturation of granule cell dendrites after mossy fiber arrival in hippocampal field CA3. Hippocampus 427, 413–427. 10.1002/hipo.10121.

Kart-Teke E, De Souza Silva MA, Huston JP, Dere E, 2006. Wistar rats show episodic-like memory for unique experiences. Neurobiol. Learn. Mem 85, 173–182. 10.1016/j.nlm.2005.10.002. [PubMed: 16290193]

Keene CS, Bladon J, Mckenzie S, Liu CD, Keefe JO, Eichenbaum H, 2016. Complementary functional organization of neuronal activity patterns in the perirhinal, lateral entorhinal, and medial entorhinal cortices. J. Neurosci 36, 3660–3675. doi:10.1523/JNEUROSCI.4368-15.2016. [PubMed: 27030753]

Kesner RP, 2013. An analysis of the dentate gyrus function. Behav. Brain Res 254, 1–7. 10.1016/j.bbr.2013.01.012. [PubMed: 23348108]

Kesner RP, 2018. An analysis of dentate gyrus function (an update). Behav. Brain Res 354, 84–91. 10.1016/j.bbr.2017.07.033. [PubMed: 28756212]

Kesner RP, Rolls ET, 2015. A computational theory of hippocampal function, and tests of the theory: new developments. Neurosci. Biobehav. Rev 48, 92–147. 10.1016/j.neubiorev.2014.11.009. [PubMed: 25446947]

Knierim JJ, Neunuebel JP, Deshmukh SS, 2014. Functional correlates of the lateral and medial entorhinal cortex: objects, path integration and local-global reference frames. Philos. Trans. R. Soc. Lond. Ser. B Biol. Sci 369, 20130369. 10.1098/rstb.2013.0369. [PubMed: 24366146]

Kuruvilla MV, Ainge JA, 2017. Lateral entorhinal cortex lesions impair local spatial frameworks. Front. Syst. Neurosci 11, 1–12. 10.3389/fnsys.2017.00030. [PubMed: 28154528]

Langston RF, Stevenson CH, Wilson CL, Saunders I, Wood ER, 2010. The role of hippocampal subregions in memory for stimulus associations. Behav. Brain Res 215, 275–291. 10.1016/j.bbr.2010.07.006. [PubMed: 20633579]

Lavenex P, Amaral DG, 2000. Hippocampal-neocortical interaction: a hierarchy of associativity. Hippocampus 10, 420–430. [PubMed: 10985281]

Leranth C, Petnehazy O, MacLusky NJ, 2003. Gonadal hormones affect spine synaptic density in the CA1 hippocampal subfield of male rats. J. Neurosci 23, 1588–1592 (doi:23/5/1588, pii). [PubMed: 12629162]

Leranth C, Hajszan T, MacLusky NJ, 2004. Androgens increase spine synapse density in the CA1 hippocampal subfield of ovariectomized female rats. J. Neurosci 24, 495–499. 10.1523/JNEUROSCI.4516-03.2004. [PubMed: 14724248]

Lonstein JS, Quadros PS, Wagner CK, 2001. Effects of neonatal RU486 on adult sexual, parental, and fearful behaviors in rats. Behav. Neurosci 115, 58–70. [PubMed: 11256453]

Meaney MJ, Sapolsky RM, McEwen BS, 1985. The development of the glucocorticoid receptor system in the rat limbic brain. I ontogeny and autoregulation. Dev. Brain Res 18, 159–164. 10.1007/s00330-011-2364-3.

Morris AM, Weeden CS, Churchwell JC, Kesner RP, 2013. The role of the dentate gyrus in the formation of contextual representations. Hippocampus 23, 162–168. 10.1002/hipo.22078. [PubMed: 23034739]

Mouton PR, Price DL, Walker LC, 1997. Empirical assessment of synapse numbers in primate neocortex. J. Neurosci. Methods 75, 119–126. 10.1016/S0165-0270(97)00058-7. [PubMed: 9288643]

Mukai H, Kimoto T, Hojo Y, Kawato S, Murakami G, Higo S, Hatanaka Y, Ogiue-Ikeda M, 2010. Modulation of synaptic plasticity by brain estrogen in the hippocampus. Biochim. Biophys. Acta Gen. Subj 1800, 1030–1044. 10.1016/j.bbagen.2009.11.002.

Newell AJ, Lalitsasivimol D, Willing J, Gonzales K, Waters EM, Milner TA, McEwen BS, Wagner CK, 2018. Progesterone receptor expression in cajal-retzius cells of the developing rat dentate gyrus: potential role in hippocampus-dependent memory. J. Comp. Neurol 526, 2285–2300. 10.1002/cne.24485. [PubMed: 30069875]

Niu S, Yabut O, D'Arcangelo G, 2008. The reelin signaling pathway promotes dendritic spine development in hippocampal neurons. J. Neurosci 28, 10339–10348. 10.1523/JNEUROSCI.1917-08.2008. [PubMed: 18842893]

Paxinos G, Watson C, 1998. The Rat Brain in Stereotaxic Coordinates Academic Press, San Diego, San Diego.

Paxinos G, Ashwell KWS, Tork I, 1994a. Atlas of the Developing Nervous System, 2ed. Academic Press, SanDiego.

Paxinos G, Ashwell KWS, Tork I, 1994b. Atlas of the Developing Rat Nervous System Academic Press, San Diego, San Diego.

Pujadas L, Gruart A, Bosch C, Delgado L, Teixeira CM, Rossi D, de Lecea L, Martinez A, Delgado-Garcia JM, Soriano E, 2010. Reelin regulates postnatal neurogenesis and enhances spine hypertrophy and long-term potentiation. J. Neurosci 30, 4636–4649. 10.1523/JNEUROSCI.5284-09.2010. [PubMed: 20357114]

Rahimi O, Claiborne BJ, 2007. Morphological development and maturation of granule neuron dendrites in the rat dentate gyrus. Prog. Brain Res 163, 167–181. 10.1016/S0079-6123(07)63010-6. [PubMed: 17765718]

Rossetti MF, Varayoud J, Andreoli MF, Stoker C, Luque EH, Ramos JG, 2017. Sex- and age-associated differences in episodic-like memory and transcriptional regulation of hippocampal steroidogenic enzymes in rats. Mol. Cell. Endocrinol 1–11 10.1016/j.mce.2017.11.001.

Sapolsky RM, Meaney MJ, 1986. Maturation of the adrenocortical stress response: neuroendocrine control mechanisms and the stress hyporesponsive period. Brain Res. Rev 11, 65–76. 10.1007/s00330-011-2364-3.

Scoville WB, Milner B, 1957. Loss of recent memory after bilateral hippocampal lesions. J. Neurol. Neurosurgey, Psychiatry 20, 11–21.

Supèr H, Martínez A, Del Río JA, Soriano E, 1998. Involvement of distinct pioneer neurons in the formation of layer-specific connections in the hippocampus. J. Neurosci 18, 4616–4626. [PubMed: 9614236]

Tamamaki N, 1999. Development of afferent fiber lamination in the infrapyramidal blade of the rat dentate gyrus. J. Comp. Neurol 266, 257–266.

Tulving E, 2002. Episodic memory: from mind to brain. Annu. Rev. Psychol 53, 1–25. [PubMed: 11752477]

Van Cauter T, Camon J, Alvernhe A, Elduayen C, Sargolini F, Save E, 2013. Distinct roles of medial and lateral entorhinal cortex in spatial cognition. Cereb. Cortex 23, 451–459. 10.1093/cercor/bhs033. [PubMed: 22357665]

Vargha-Khadem F, Gadian DG, Watkins KE, Connelly A, Van Paesschen W, Mishkin M, 1997. Differential effects of early hippocampal pathology on episodic and semantic memory. Science (80-.) 277, 376–380.

Wilson DIG, Langston RF, Schlesiger MI, Wagner M, Watanabe S, Ainge JA, 2013a. Lateral entorhinal cortex is critical for novel object-context recognition. Hippocampus 23, 352–366. 10.1002/hipo.22095. [PubMed: 23389958]

Wilson DIG, Watanabe S, Milner H, Ainge JA, 2013b. Lateral entorhinal cortex is necessary for associative but not nonassociative recognition memory. Hippocampus 23, 1280–1290. 10.1002/hipo.22165. [PubMed: 23836525]

Witter MP, 2007. The perforant path: projections from the entorhinal cortex to the dentate gyrus. Prog. Brain Res 163, 43–61. 10.1016/S0079-6123(07)63003-9. [PubMed: 17765711]

Witter MP, Naber PA, von Haeften T, Machielsen WCM, Rombouts SARB, Barkhof F, Scheltens P, Lopes da Silva FH, 2000. Cortico-hippocampal communication by way of parallel parahippocampal-subicular pathways. Hippocampus 10, 398–410. 10.1680/udap.2010.163. [PubMed: 10985279]

Woolley CS, 1998. Estrogen-mediated structural and functional synaptic plasticity in the female rat hippocampus. Horm. Behav 34, 140–148. 10.1006/hbeh.1998.1466. [PubMed: 9799624]

Yoganarasimha D, Rao G, Knierim JJ, 2011. Lateral entorhinal neurons are not spatially selective in cue-rich environments. Hippocampus 21, 1363–1374. 10.1016/j.pestbp.2011.02.012.Investigations. [PubMed: 20857485]

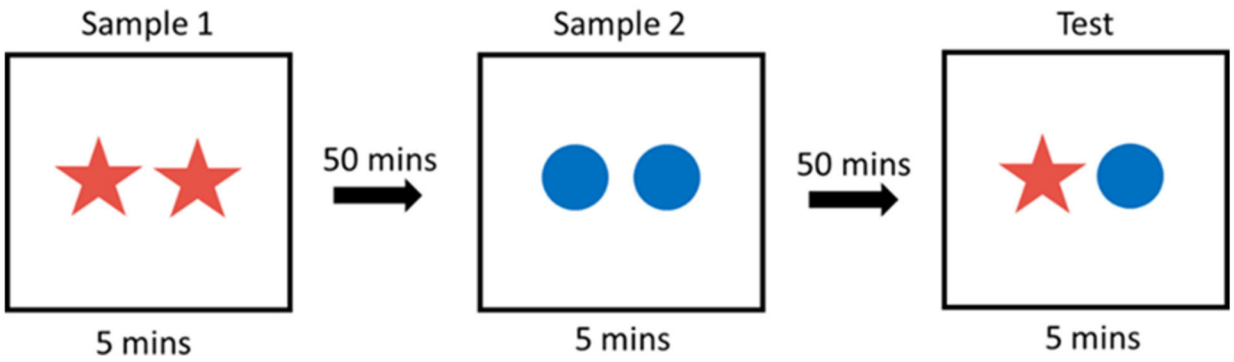

Fig. 1.

Relative Recency behavioral task. Rats are presented with two identical objects for 5 mins in two consecutive Sample sessions separated by two 50 min inter-trial intervals. In the Test session, the animals are presented with one object from each sample. This design presents the animal with two objects which vary on two components of episodic-like memory: what (object identity) and when (distant vs recent).

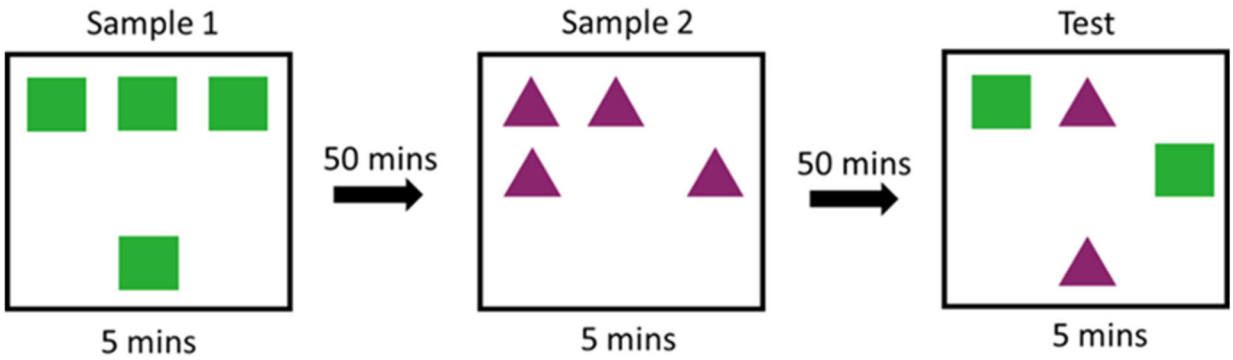

Fig. 2.

Episodic-like Memory behavioral task. Rats are presented with four identical objects for 5 mins in two consecutive Sample sessions separated by a 50 min inter-trial interval. This arrangement creates items that vary temporally (distant vs recent). After another 50 min the animals are presented with 2 copies of both the distant and recent objects, one of which has been moved to a novel location (stationary vs displaced). This design presents rats in the test session with four objects which vary on all three components of episodic-like memory: what (object identity), when (distant vs recent), and where (stationary vs displaced).

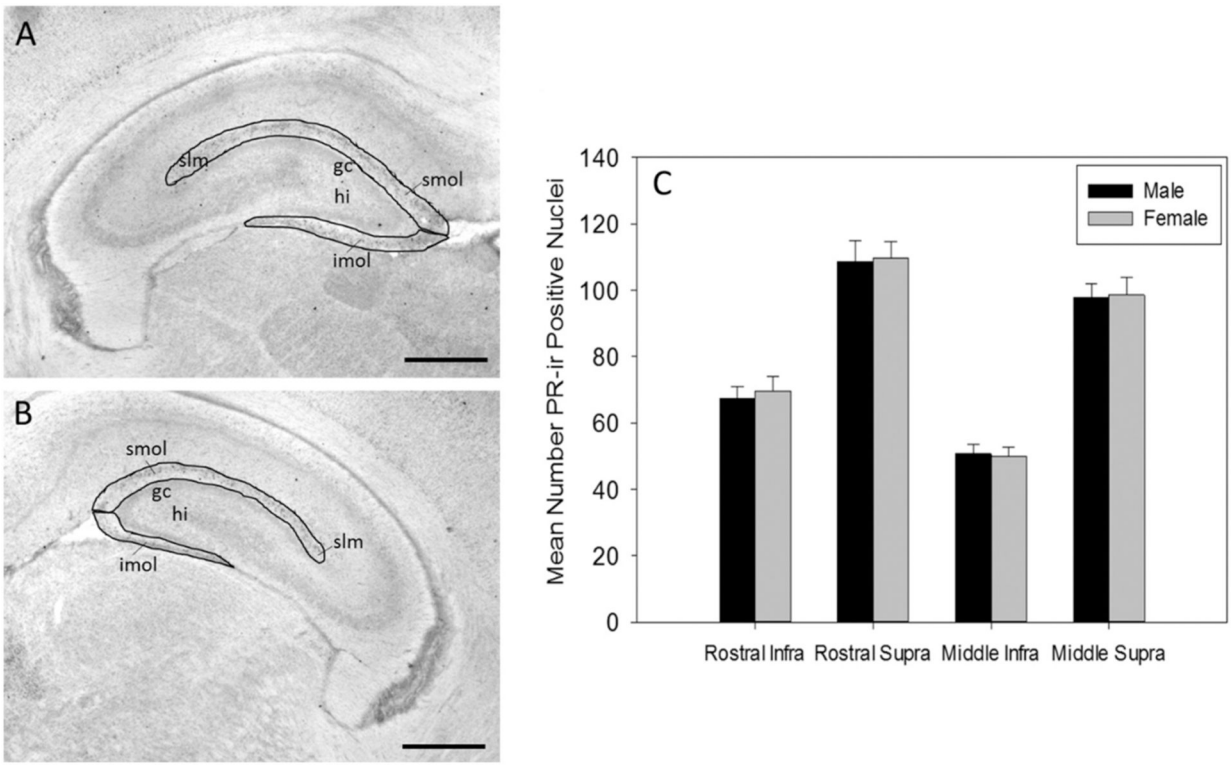

Fig. 3.

Progesterone receptor immunoreactivity in male and female dentate gyrus. Representative image of (A) rostral dentate gyrus and (B) middle dentate gyrus highlighting regions of interest where PR was quantified (gc (granule cell layer), hi (hilus), imol (infrapyramidal molecular layer), slm (stratum lacunosum moleculare), smol (suprapyramidal molecular layer)) (scale bar = 500 μm). (C) The mean number of progesterone receptor immunoreactive (PR-ir) cell nuclei in the rostral and middle infrapyramidal and suprapyramidal blades of the outer molecular layer of the dentate gyrus (DG) of male (N = 23) and female (N = 23) rats at postnatal day 7.

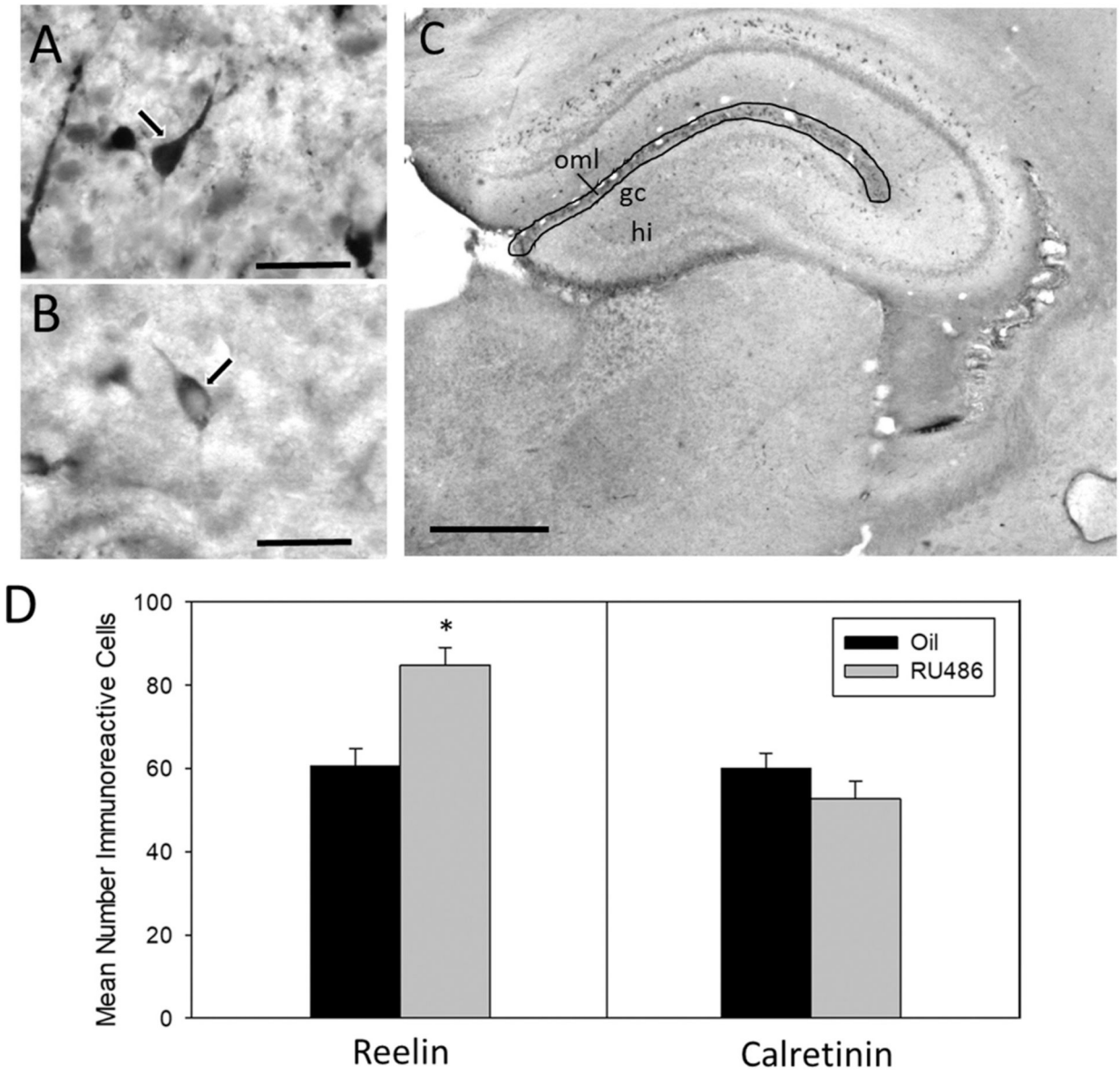

Fig. 4.

Number of reelin and calretinin cells in suprapyramidal outer MOL of P7 males. (A) Representative image of Calretinin-ir cell in suprapyramidal layer of MOL at P7 taken at 100× magnification (scale bar = 30 μm). Arrow illustrates distinctive 'tadpole-like' morphology indicative of Cajal-Retzius cells. (B) Representative image of Reelin –ir in suprapyramidal layer of MOL at P7 taken at 100× magnification (scale bar = 30 μm). (C) Representative image of dorsal hippocampus indicating region of quantification of reelin and calretinin-ir (gc (granule cell layer), hi (hilus), oml (outer molecular layer)) (scale bar = 500 μm). (D) Mean number (±sem) of reelin immunoreactive (ir) cells and calretinin-ir cells in the suprapyramidal outer molecular layer of the dentate gyrus at postnatal day 7 in RU486- or oil-treated male rats (*significantly different from controls, $p < 0.05$).

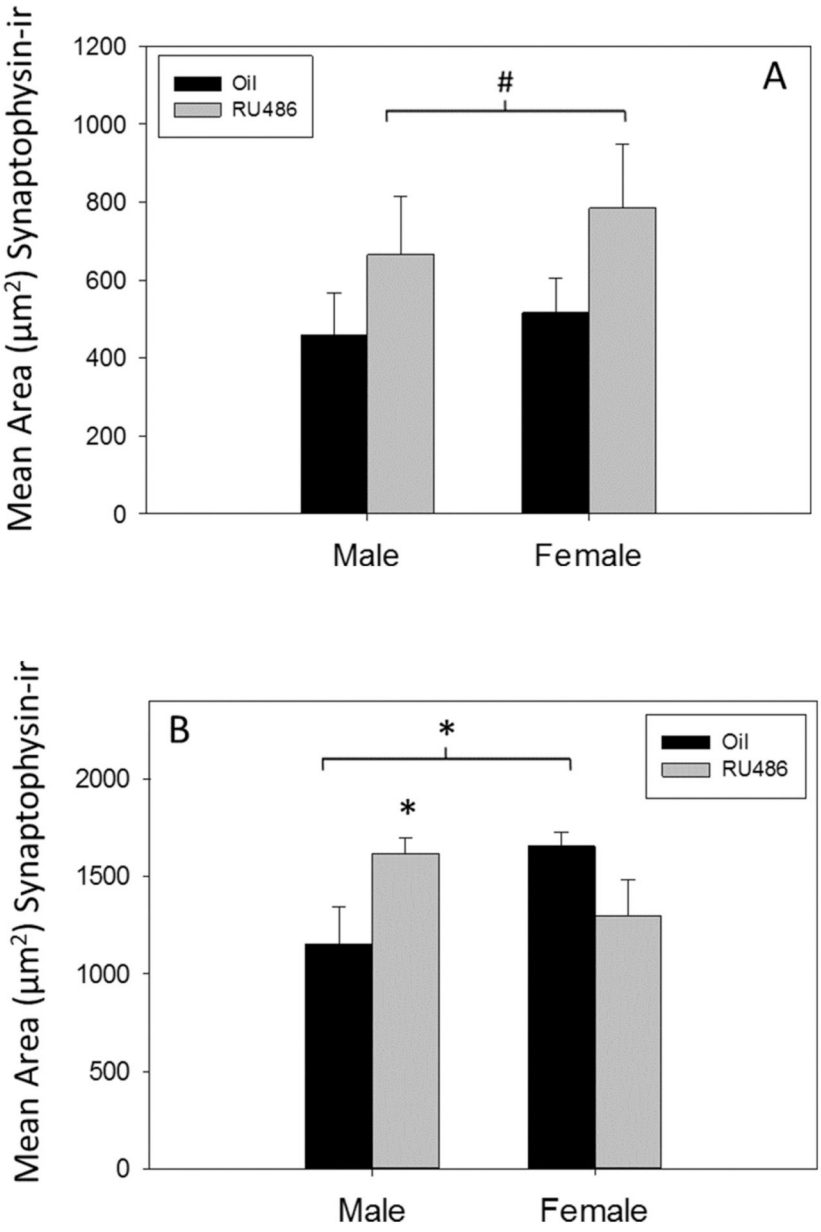

Fig. 5.

Synaptophysin immunoreactivity in postnatal day 7 dentate gyrus. The mean (±sem) relative total amount of synaptophysin-ir (area (μm^2) covered by pixels) in RU486- or oil-treated males and females at postnatal day 7 in (A) the infrapyramidal blade ($^{\#}p = 0.06$) or (B) the suprapyramidal blade ($^{*}p < 0.05$) of the molecular layer.

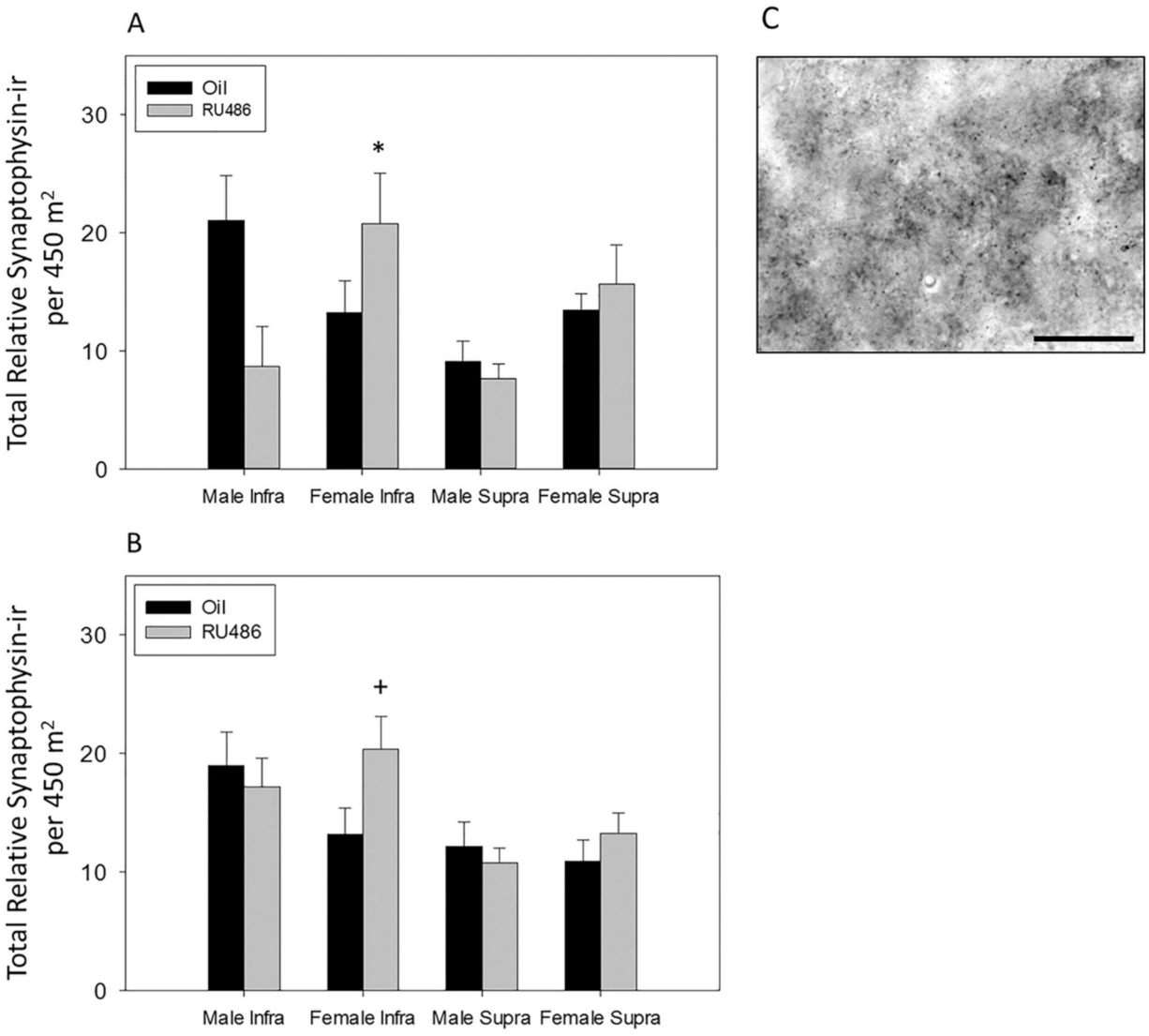

Fig. 6.

Synaptophysin immunoreactivity in postnatal day 21 dentate gyrus. Mean density of synaptophysin-ir boutons in infrapyramidal and suprapyramidal blades of the (A) rostral and (B) middle molecular layer of the dentate gyrus of P21 males and females treated with the PR antagonist, RU486, or oil. (A) RU486 treated females have significantly denser synaptophysin-ir than males (*$p < 0.05$). (B) RU486 treated females show significantly higher density of synaptophysin-ir at P21 than those treated with oil in the infrapyramidal blade ($^{+}p < 0.05$). (C) Representative of synaptophysin-ir in infrapyramidal molecular layer of dentate gyrus at P21 (scale bar = 30 μm).

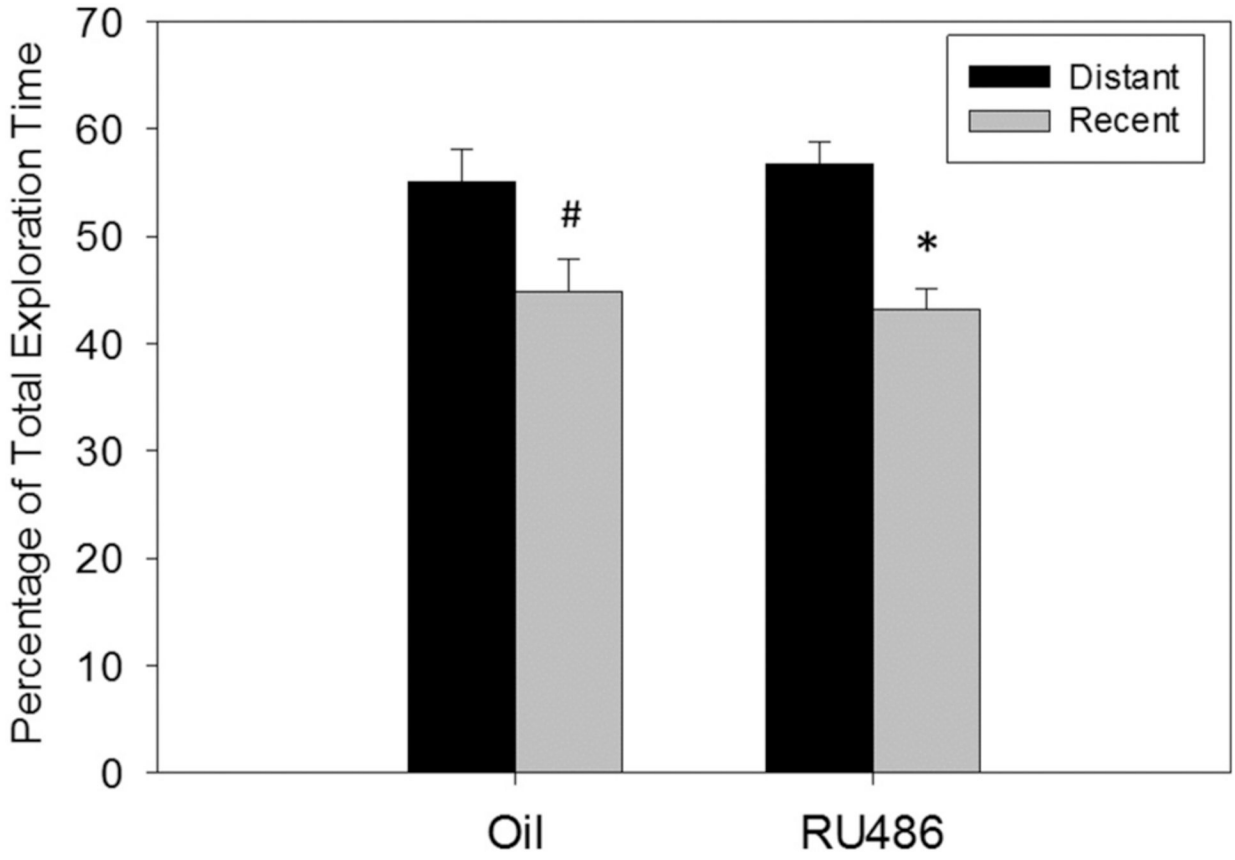

Fig. 7.

Relative Recency behavioral task. Percentage of total object exploration time of distant or recent presented objects in adult male rats treated postnatally with oil or RU486 Both groups show a preference to explore the ‘distant’ object over the ‘recent’ object (distant vs recent, #$p = 0.051$, *$p < 0.05$).

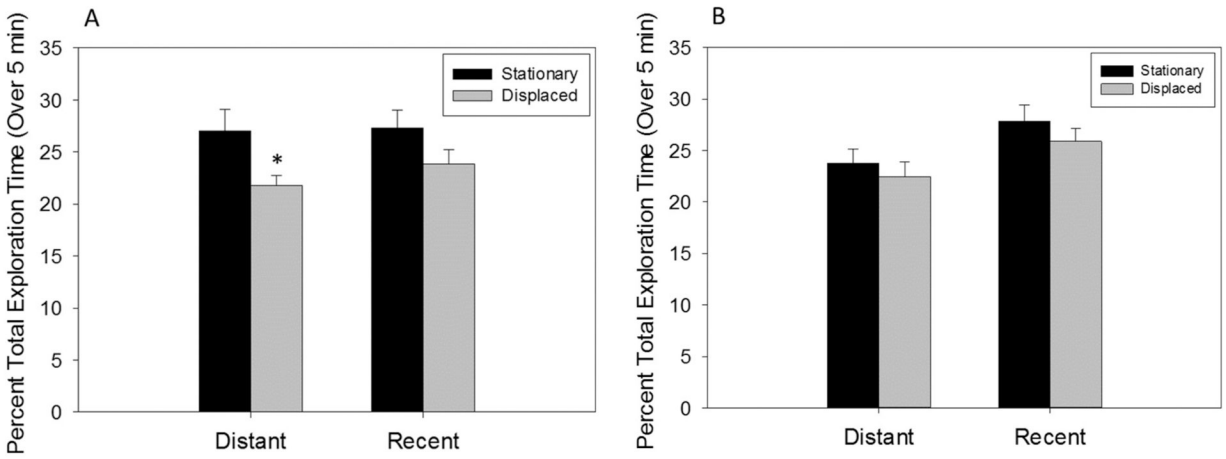

Fig. 8.

Episodic-like memory behavioral task. Object exploration time of stationary or displaced objects that were temporally distant or recent as percentage of total exploration time in adult male rats treated postnatally with (A) oil or (B) RU486. Oil treated rats prefer the temporally distant, stationary object over the temporally distant, displaced object distant stationary vs distant displaced (*$p < 0.05$). There are no significant object preferences in RU486 treated rats.